Introduction to astroparticle physics

Part 1: Andrii Neronov

Cosmic ray physics

... direct continuation of
research started by V.Hess

Gamma-ray astronomy

.... application of particle physics
methods in astronomy

Gravitational waves

Neutrino physics

* neutrino oscillations
* high-energy neutrino astronomy

Dark matter physics

... direct continuation of
research started by F.Zwicky

Particle physics in the Early Universe

... direct continuation of research started by Gamow

Reminder previous lecture

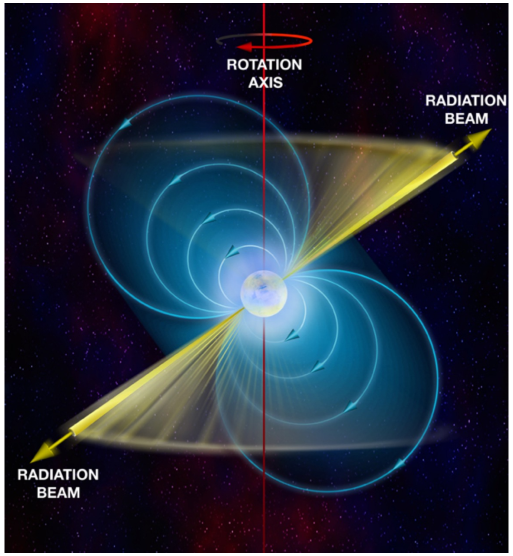

pulsars

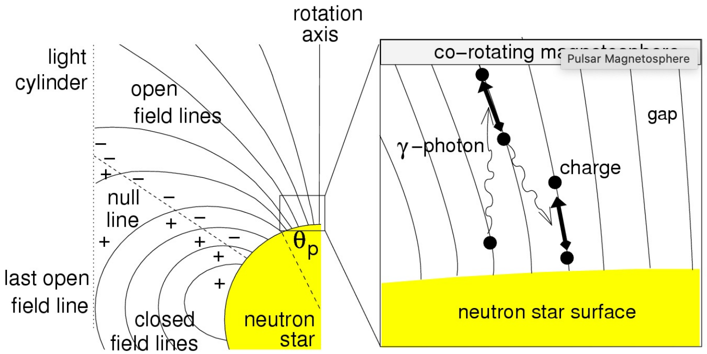

Gamma-ray bursts

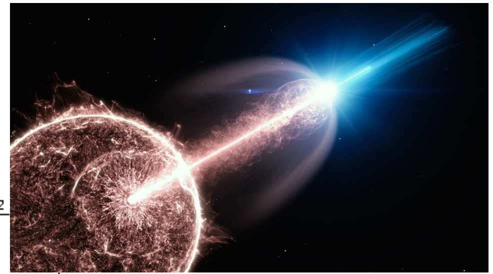

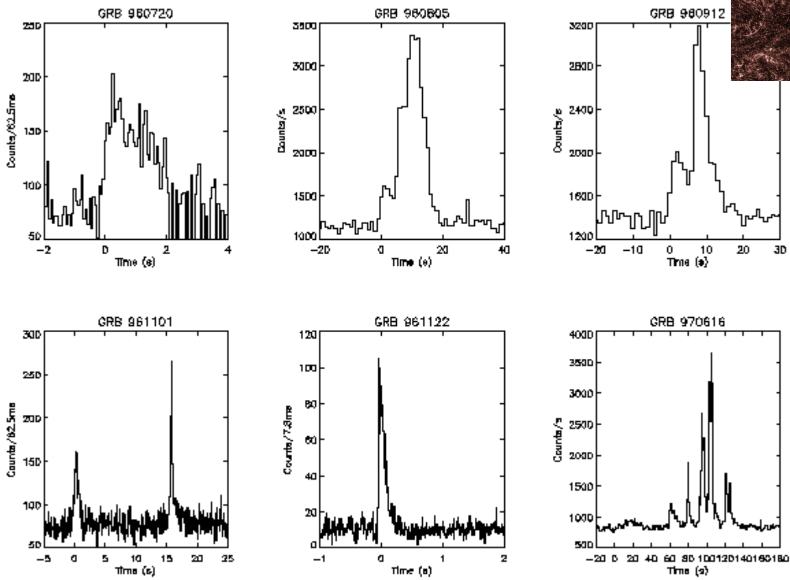

Particle accelerator near neutron star

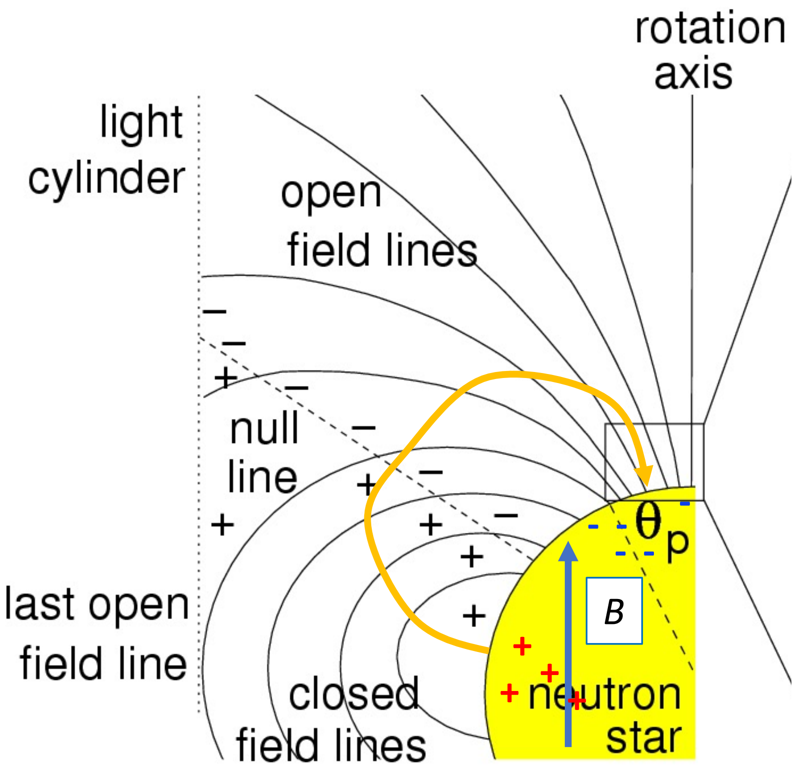

Charge separation at the surface induces quadrupole electric field outside the star. Typical electrostatic potential

$$U \sim \frac{R^2 B}{T} \sim 10^{20} \left[\frac{B}{10^{12}\ G}\right] \left[\frac{R}{10^{6}\ cm}\right]^2 \left[\frac{T}{1\ ms}\right]^{-1} V$$

“Hillas plot”: cosmic particle colliders

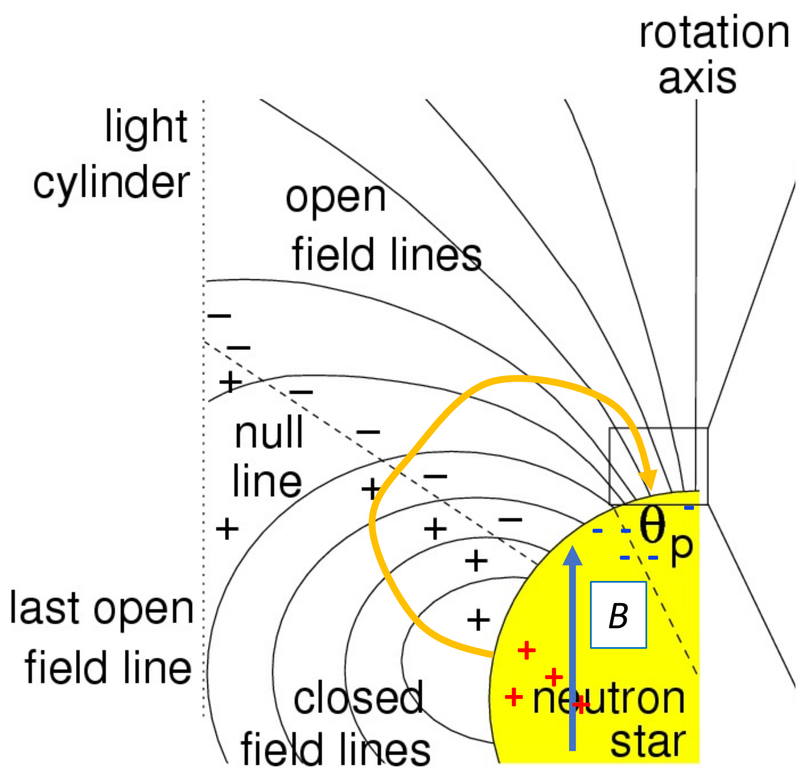

Let’s take $T \sim R/c$ (minimal possible).

$$U \sim RB$$

$$E_{max} \sim eU \sim eBR \simeq 3{\times}10^{20}\ \text{eV}$$

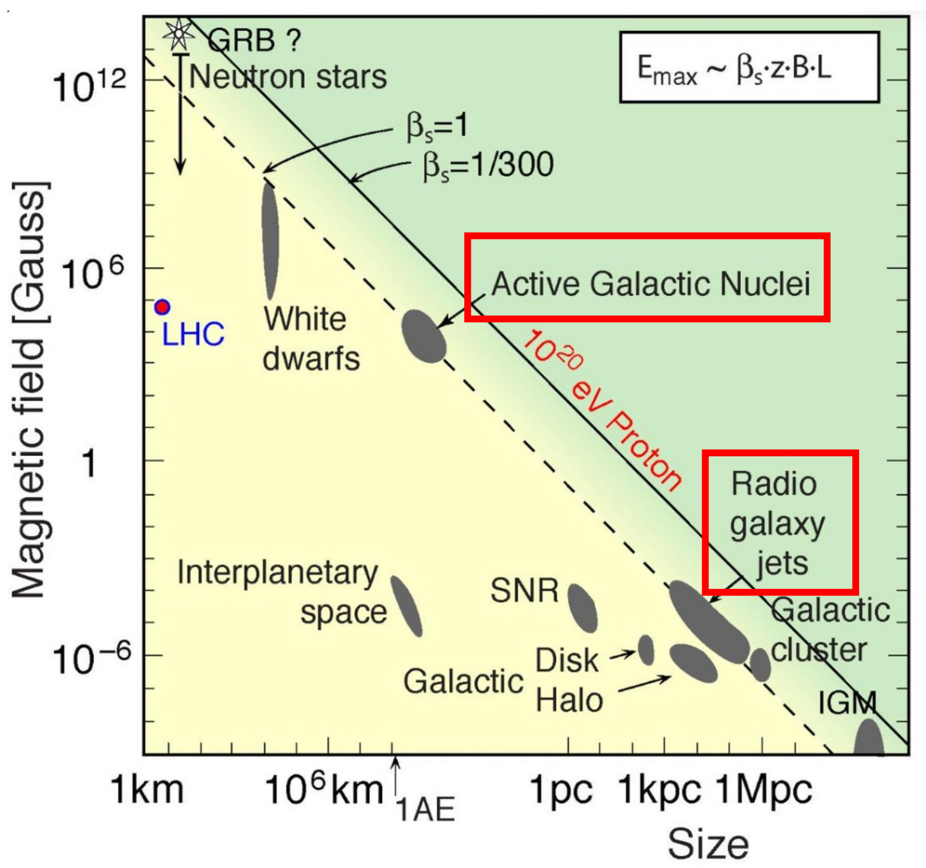

Charge separation at the surface induces quadrupole electric field outside the star. Typical electrostatic potential

$$U \sim \frac{R^2 B}{T} \sim 10^{20}\left[\frac{B}{10^{12}\ G}\right]\left[\frac{R}{10^{6}\ cm}\right]^2\left[\frac{T}{1\ ms}\right]^{-1} V$$

Highest energy particles in nature?

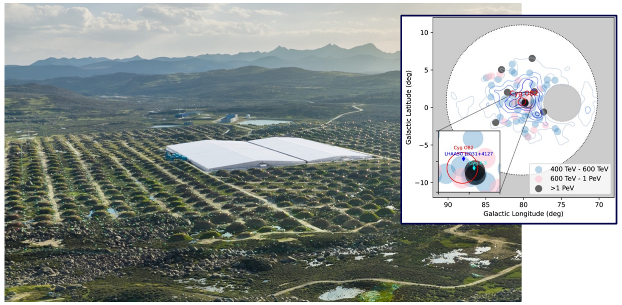

LHAASO
$> 10^3$ TeV gamma-rays

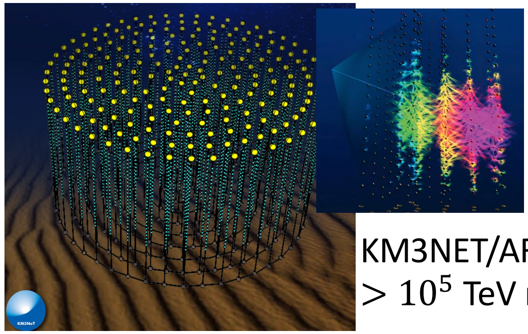

KM3NET/ARCA
$> 10^5$ TeV neutrino

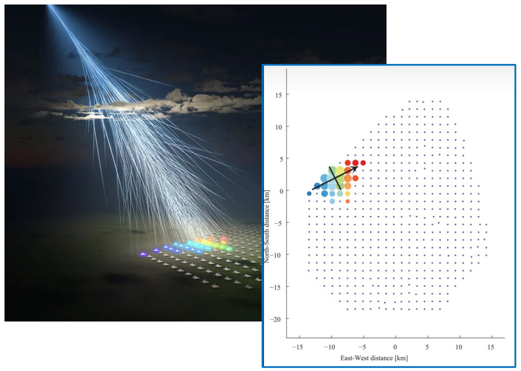

Telescope Array
2.4×10^8 TeV cosmic ray

Let's take $T \sim R/c$ (minimal possible).

$$U \sim RB$$

$$E_{max} \sim eU \sim eBR \simeq 3\times10^{20}\ \text{eV}$$

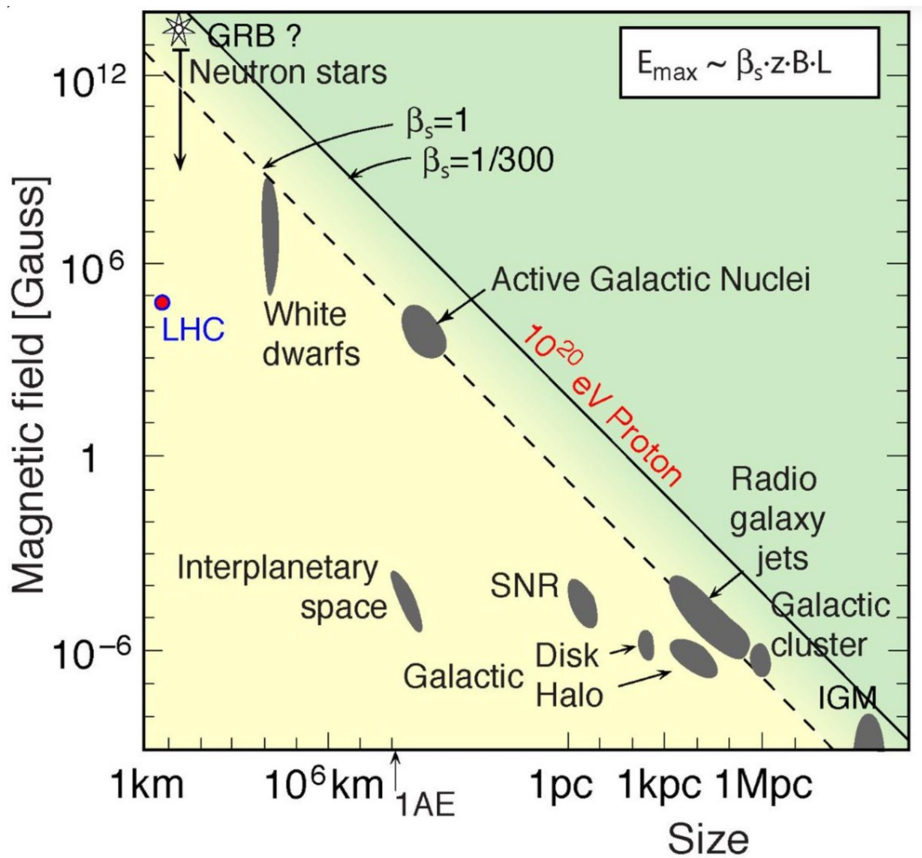

Highest energy particles in nature?

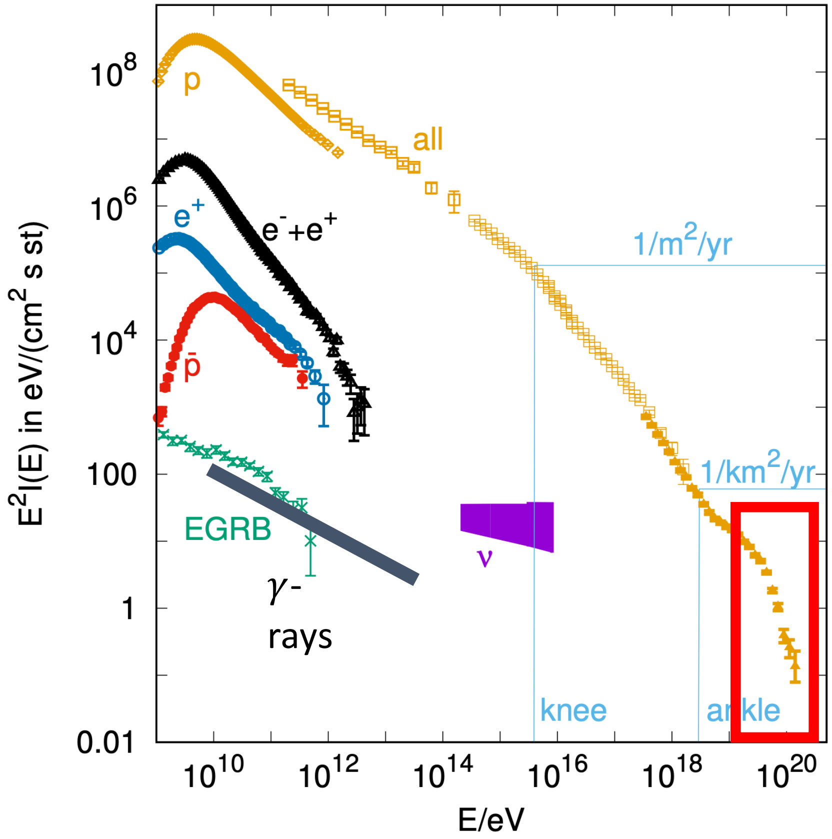

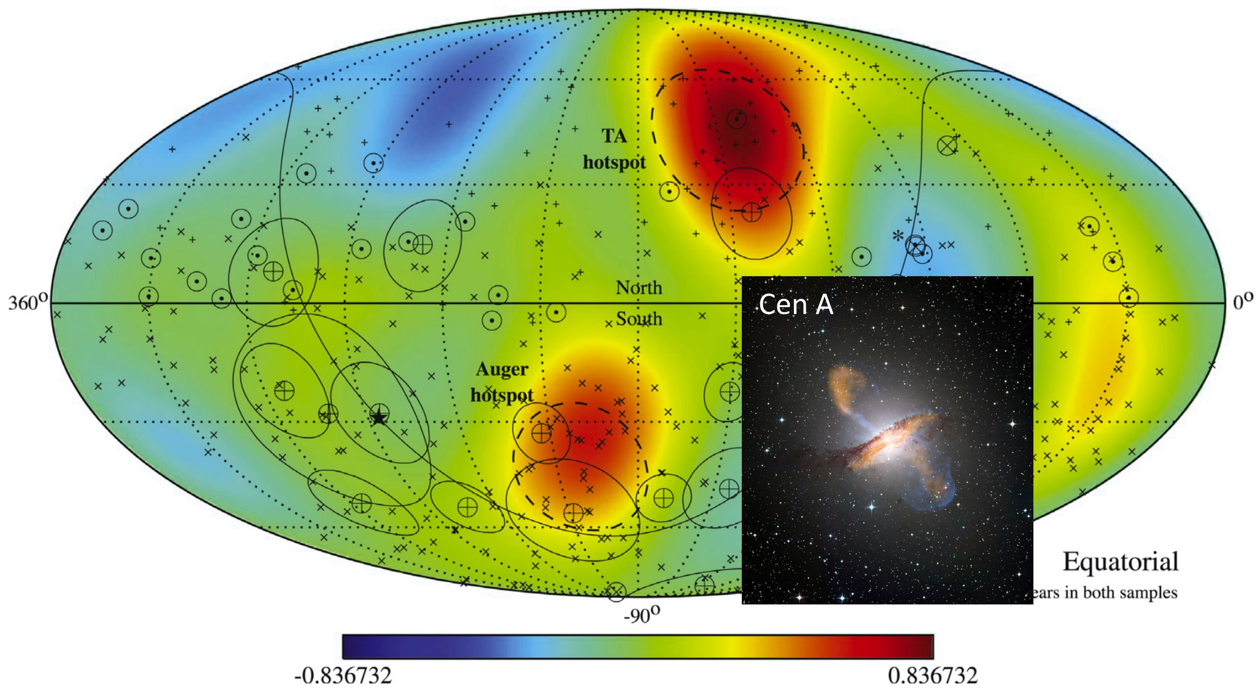

Sky map of UHECR events collected by Pierre Auger Observatory in 10 years of operation (x) and Telescope Array experiment (+) in five years of operation. Colour shows the sky map smoothed with 20 degree kernel. The two “hotspots” have post-trial p-value 1.4×10^{-2} (Auger) and 3.7×10^{-4} (Telescope Array).

Active galactic nuclei

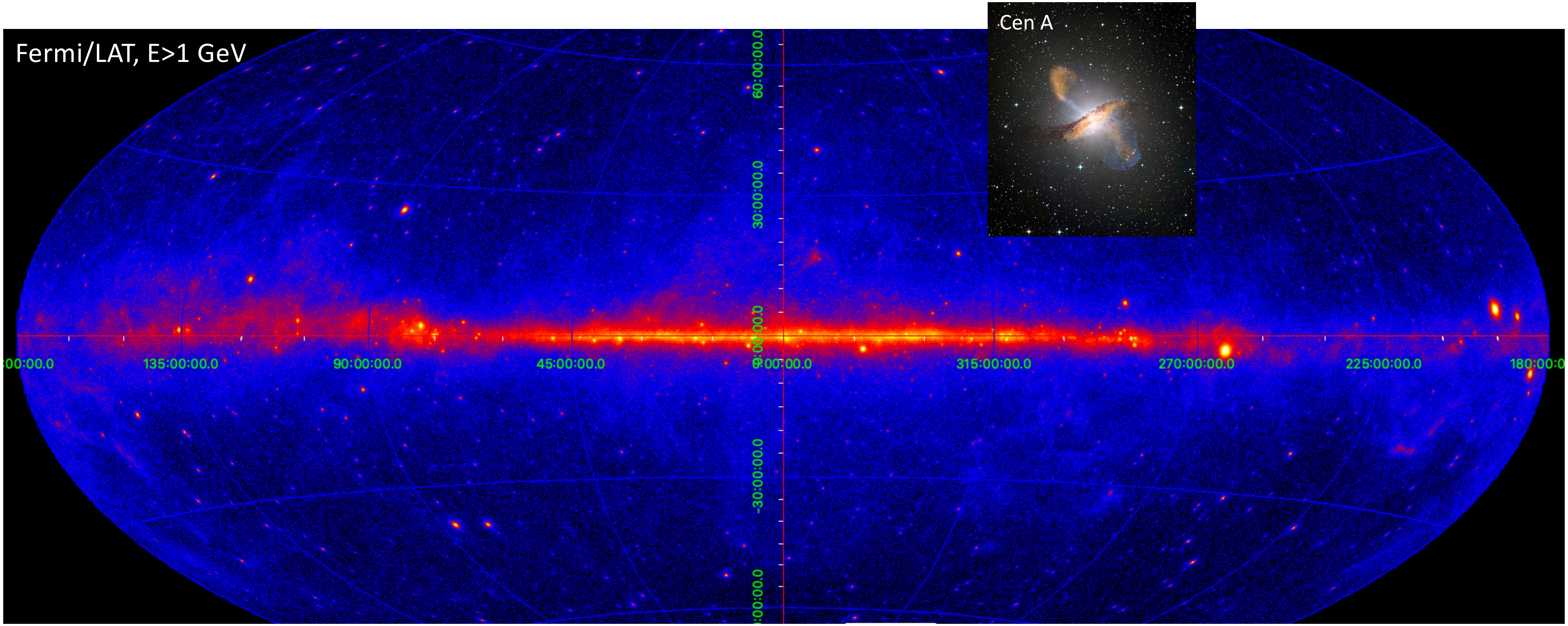

Most of the isolated gamma-ray sources outside the Galactic Plane are Active Galactic Nuclei (AGN) powered by supermassive black holes

Supermassive black holes

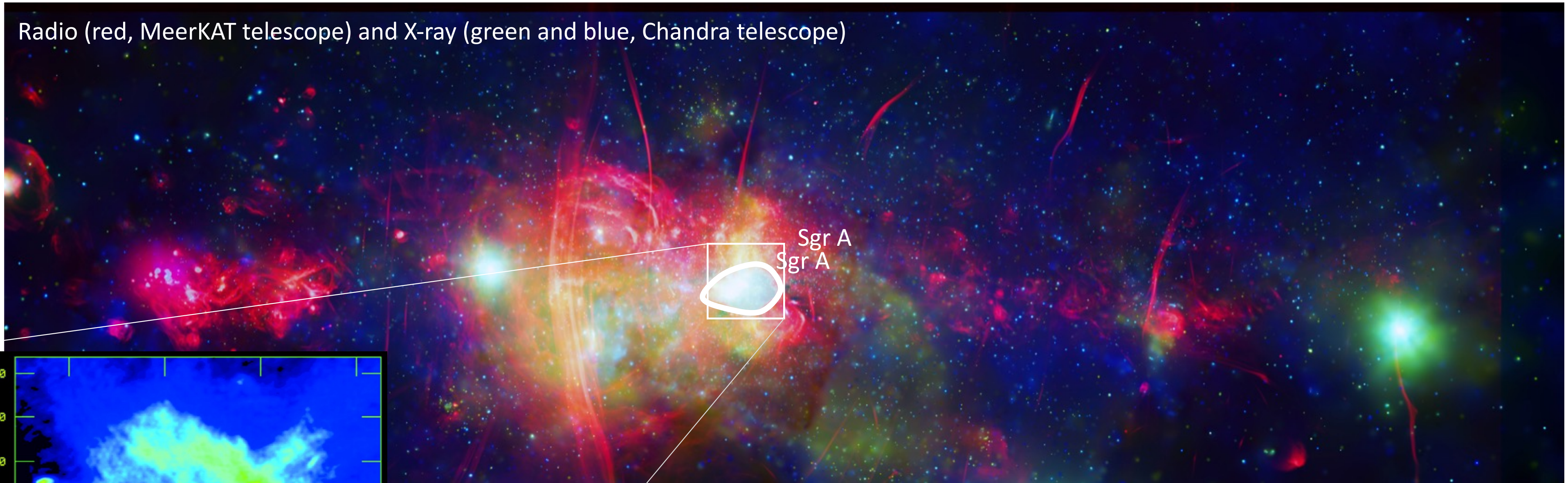

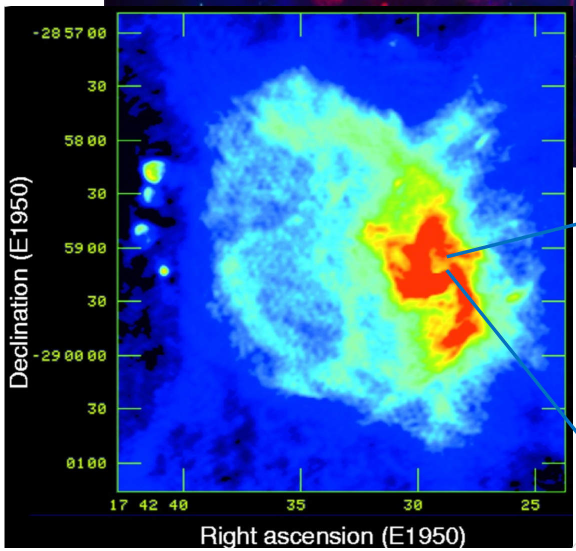

VLA telescope (radio) image of Sgr A

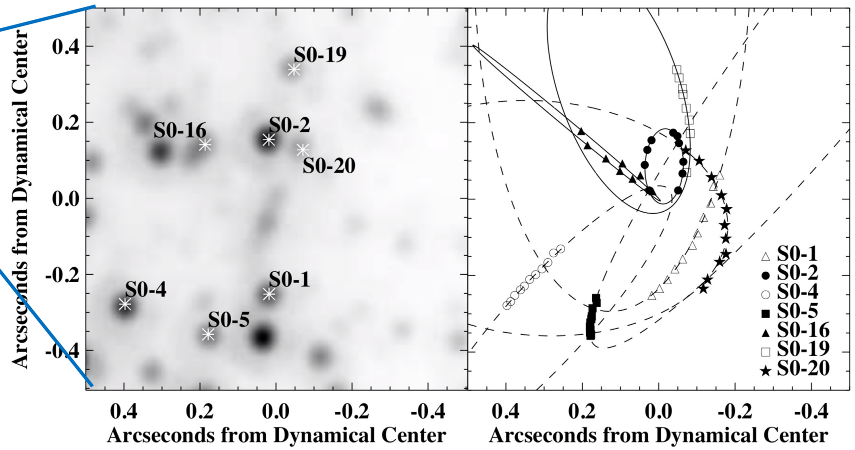

Center of the Milky Way galaxy hosts a black hole of mass $4\times10^6 M_\odot$. Its existence is established based on trajectories of stars orbiting the black hole along Keplerian orbits, at the distance $\sim 10^3$ of its gravitational radius

$$R_g = \frac{G_N M}{c^2} \simeq 1.5 \left(\frac{M}{M_\odot}\right) \text{ km}$$

This black hole is “inactive” ($L \sim 10^2 L_\odot$).

Supermassive black holes

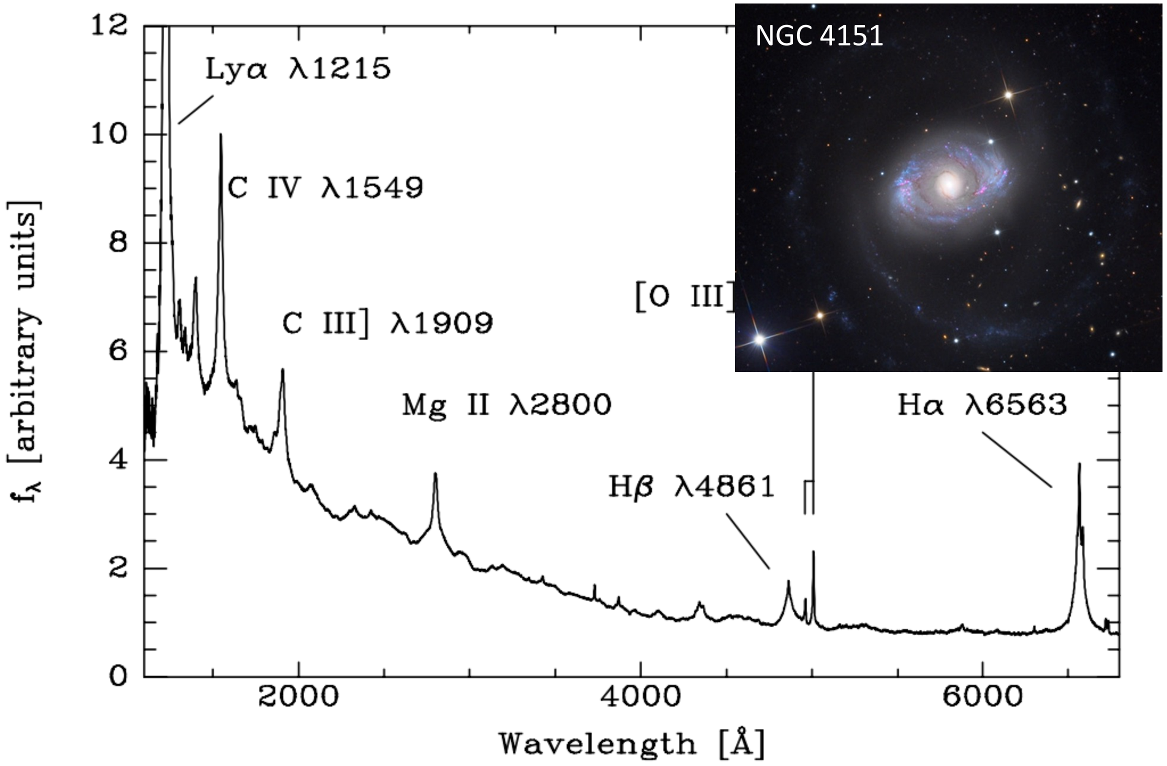

Optical-UV spectrum of active galactic nucleus.

Most of the Milky Way mass galaxies host supermassive black holes in their centers. Some of these black holes are visible as bright central sources in the galaxies.

Spectra of these sources show emission lines (rather than absorption lines, typical to stars). The lines may appear strongly broadened by the Doppler effect

$$\frac{\Delta\lambda}{\lambda} \sim \frac{v}{c}$$

produced by matter presumably with Keplerian (or virial) velocities

$$v_K = \sqrt{\frac{G_N M}{R}} \simeq 10^{-2} c \left(\frac{M}{10^8 M_\odot}\right)^{\frac{1}{2}} \left(\frac{R}{10^{15}\mathrm{m}}\right)^{-1/2}$$

The line flux is variable on short time scales. The “causality” argument implies compact size of the emission region

$$R \sim vT_{var} \sim 10^{15} \left(\frac{v}{c}\right) \left(\frac{T_{var}}{0.1\ \mathrm{yr}}\right)\ \mathrm{m}$$

Active galactic nuclei

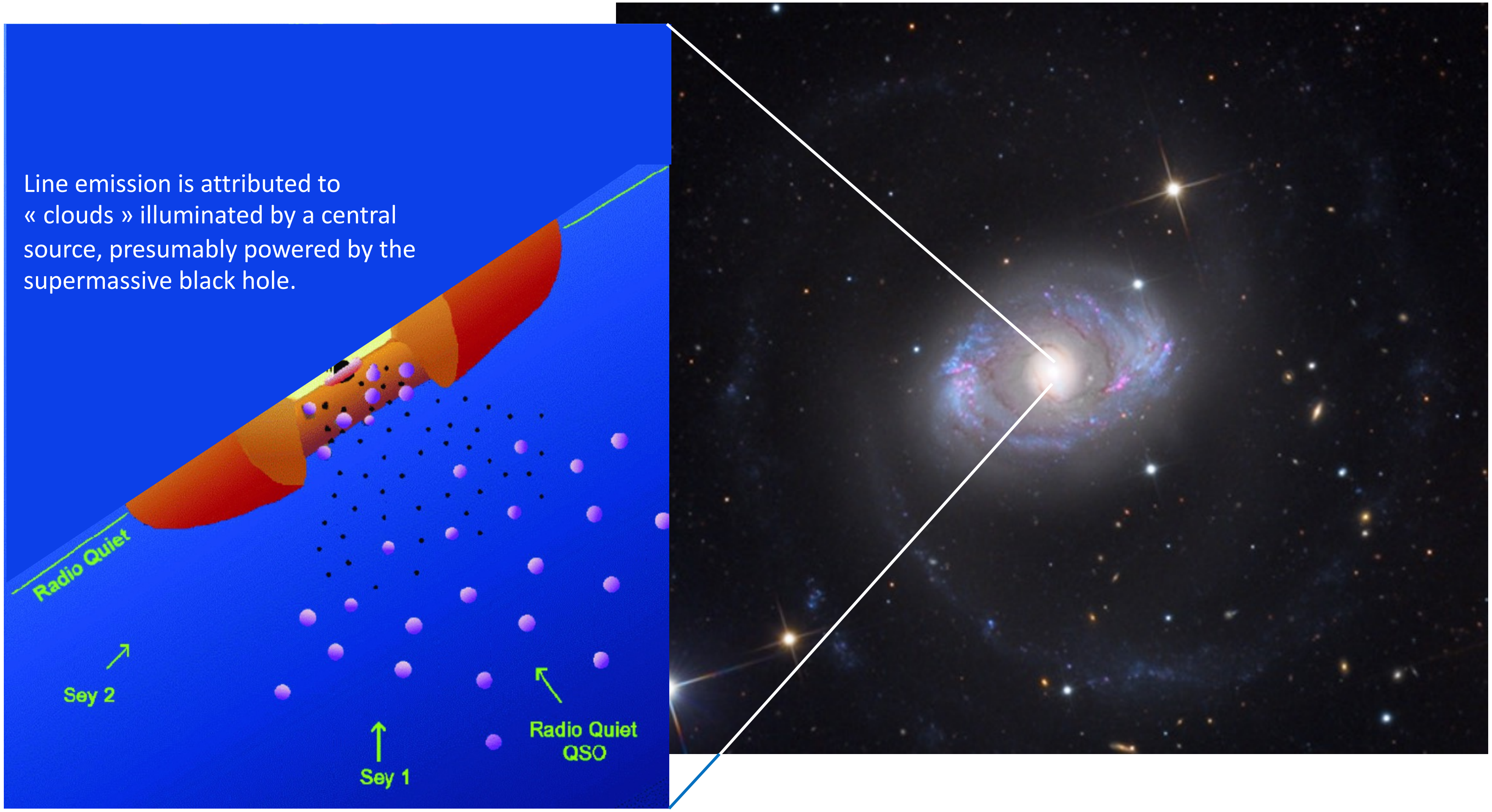

Different types of AGN

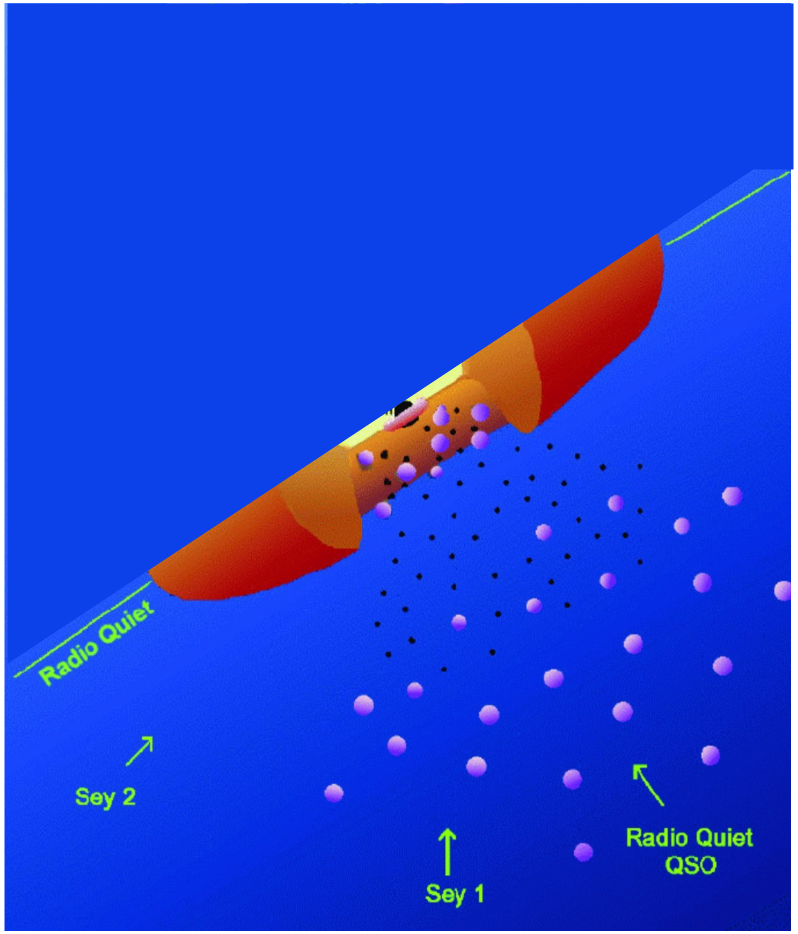

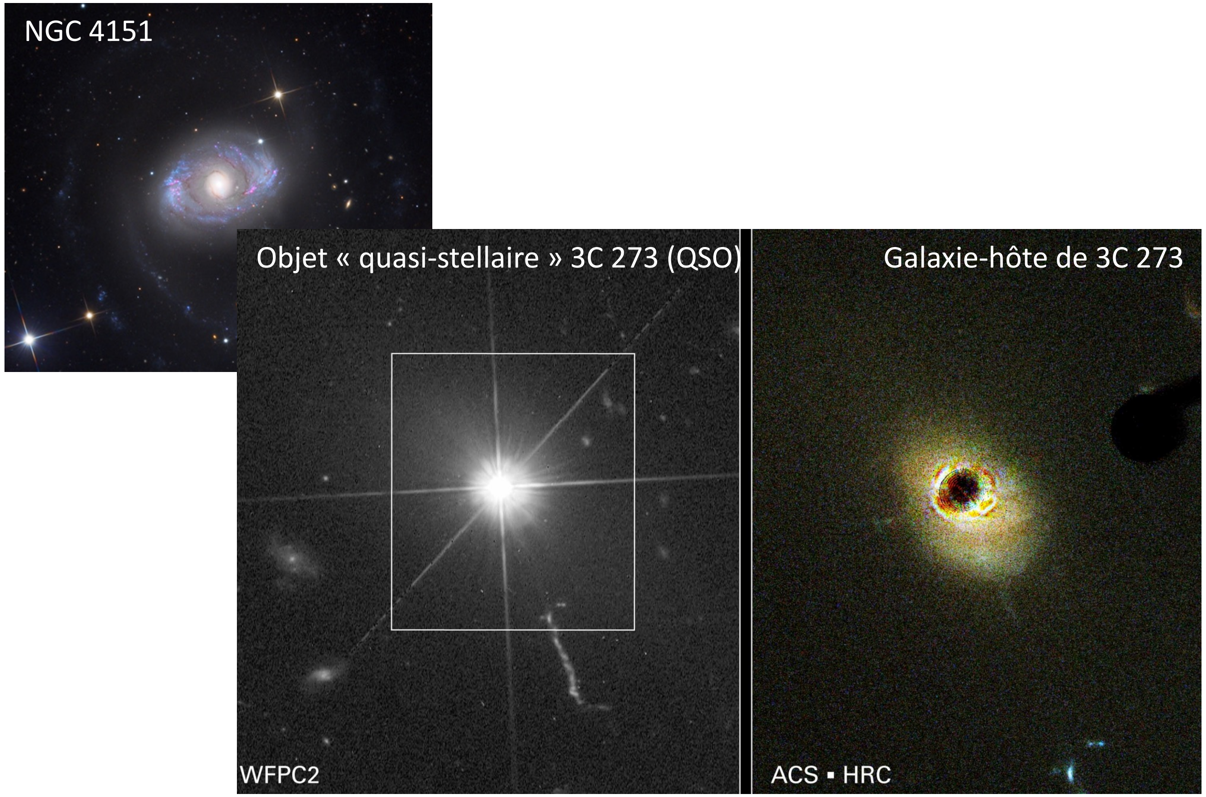

AGN luminosities can be larger than the luminosity of the whole galaxy hosting the black hole (AGN outshining their host galaxies are called “Quasi-Stellar Objects, QSO). Observational appearance of an AGN depends on the orientation of the system with respect to the line of sight.

“Radio-loud” and “radio-quiet” AGN

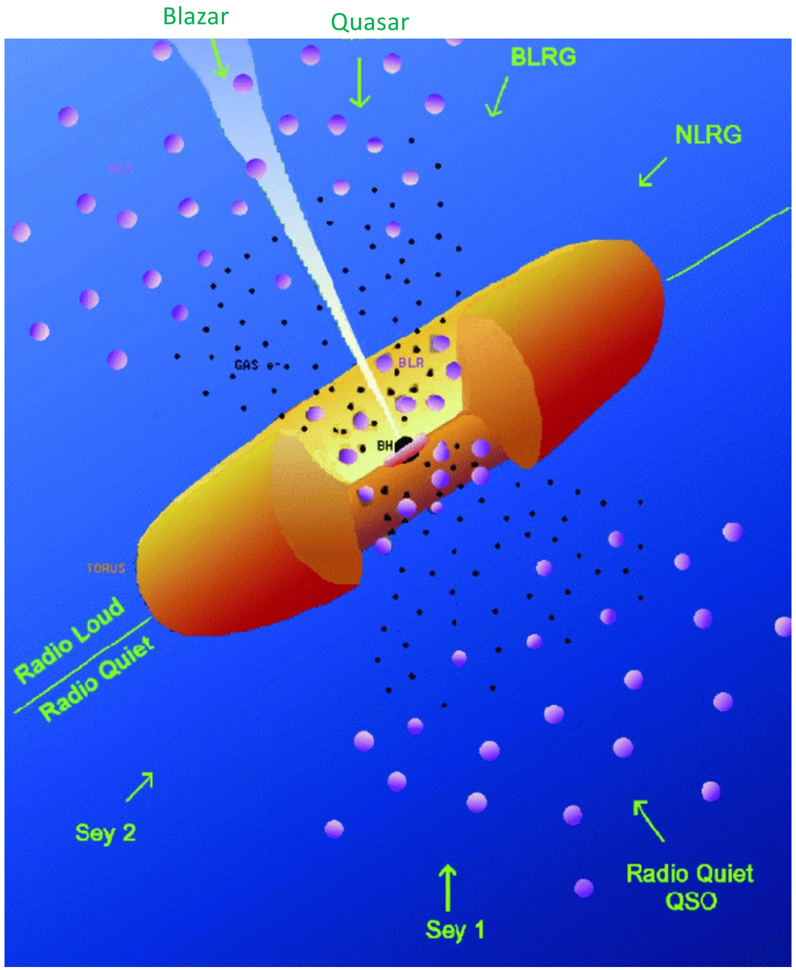

Some 10% of AGN eject directed flows of relativistic particles, jets.
Jet lengths can reach kpc-Mpc scale (larger than the size of the AGN host galaxies). Synchrotron emission from the jets is traced by radio telescopes, hence the name of this AGN class, “radio-loud”.

Strong Doppler effect increases the apparent brightness of radio-loud AGN with jets aligned along the line of sight. Such radio-loud AGN are called “blazars”.

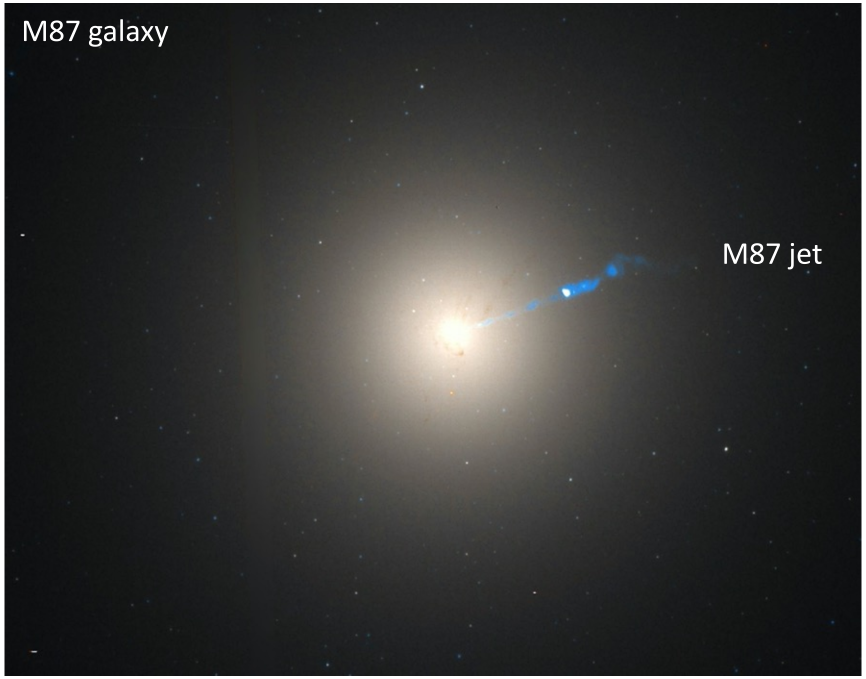

Jets

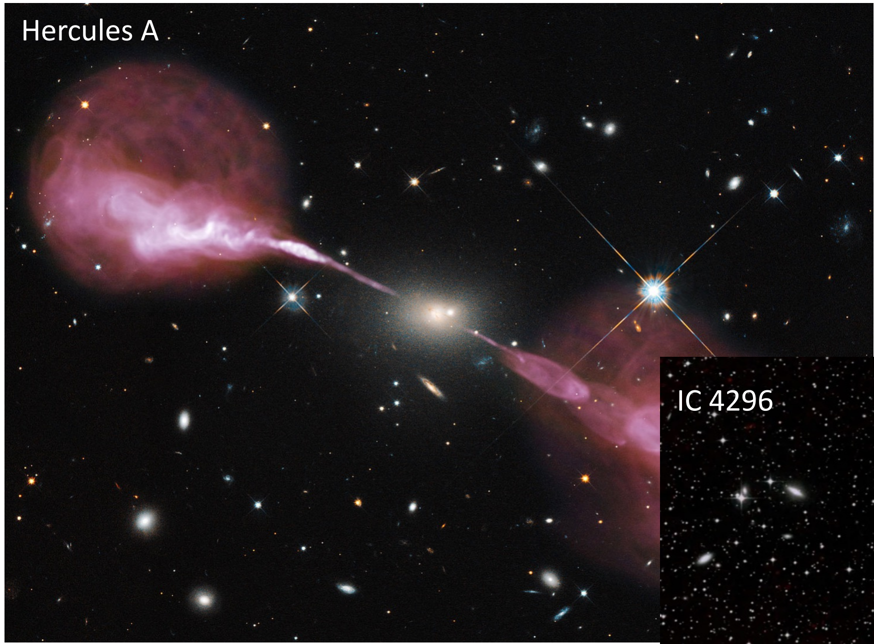

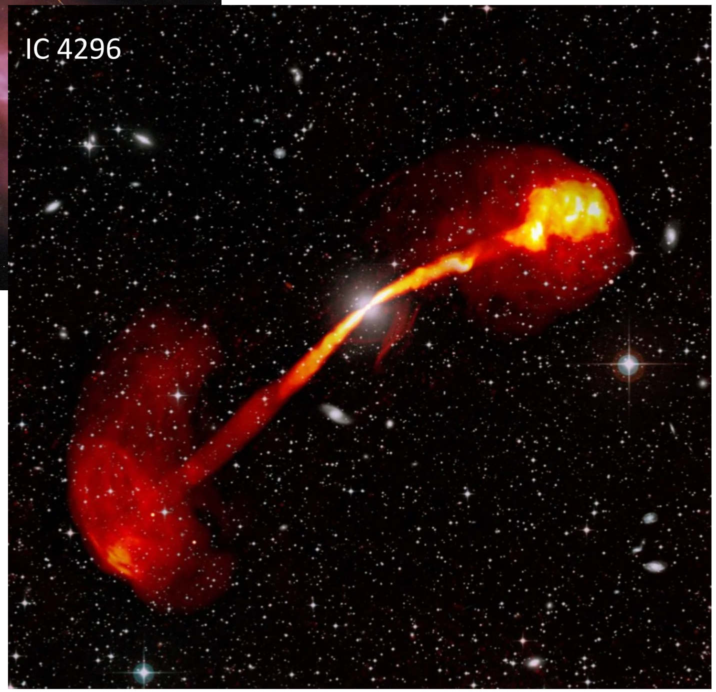

Jets

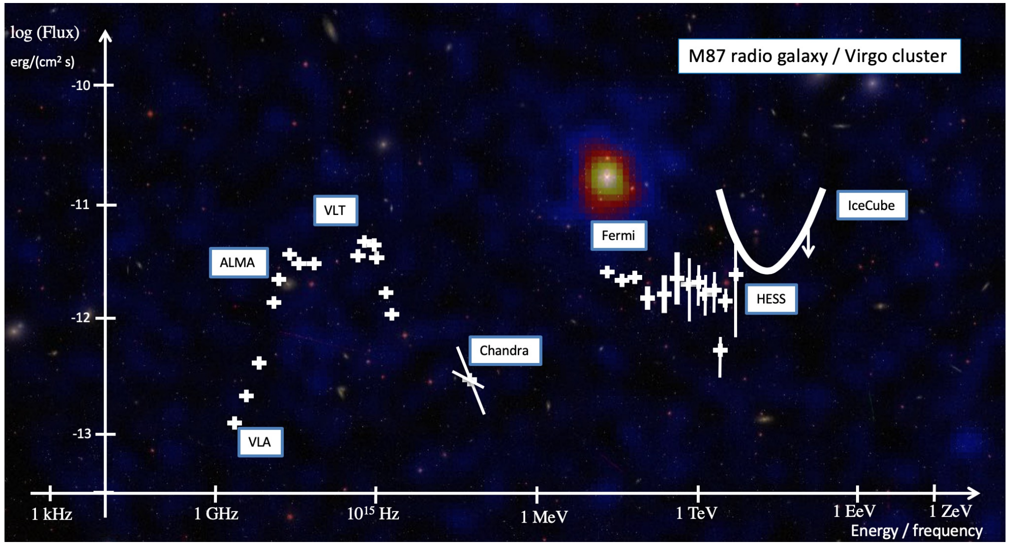

Radio-loud AGNs are visible through all electromagnetic astronomical windows: radio, infrared, visible, UV, X-rays, gamma rays, very high energy gamma rays.

Their "non-thermal" electromagnetic emission is produced by particles accelerated near the supermassive black hole and/or in the jet. These particles emit synchrotron radiation in the radio-X-ray band and inverse Compton scattering emission in gamma rays.

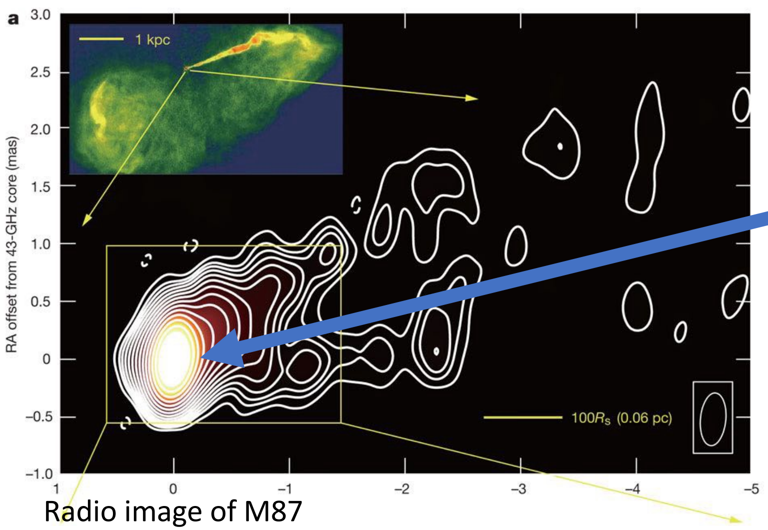

Radio image of M87

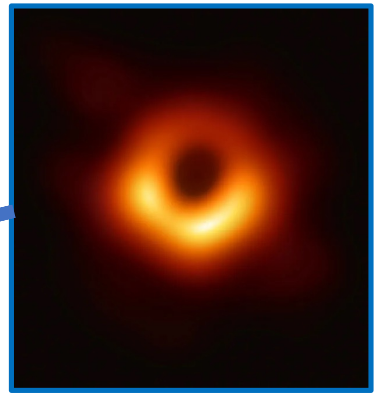

High-resolution radio image of M87 black hole

Stellar mass black holes

Black holes and neutron stars in binary stellar systems also can accrete matter (from a companion star).

Black holes in X-ray binaries can have masses reaching $(10-30)M_{\odot}$. This suggests that the compact objects formed by the collapsed cores of massive stars (of initial mass $M \simeq M_{Ch} \simeq 1.4M_{\odot}$) can experience intense growth through accretion of stellar material (not ejected by the supernova explosion).

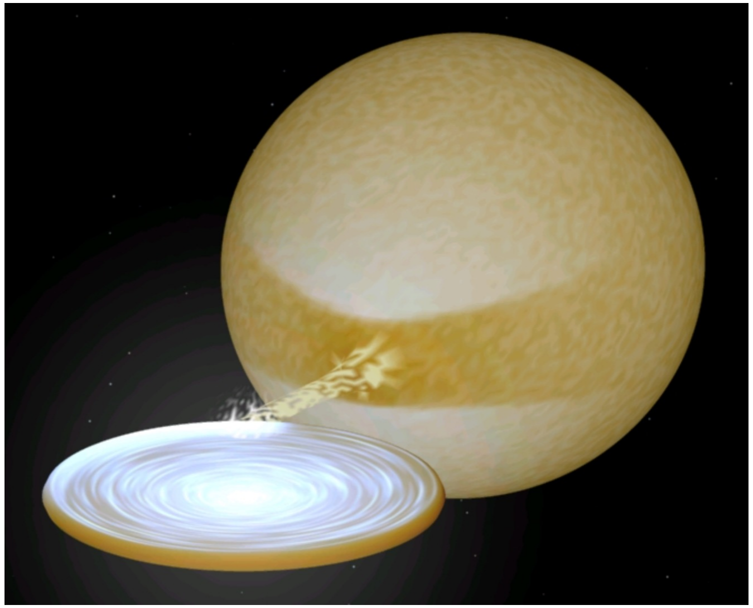

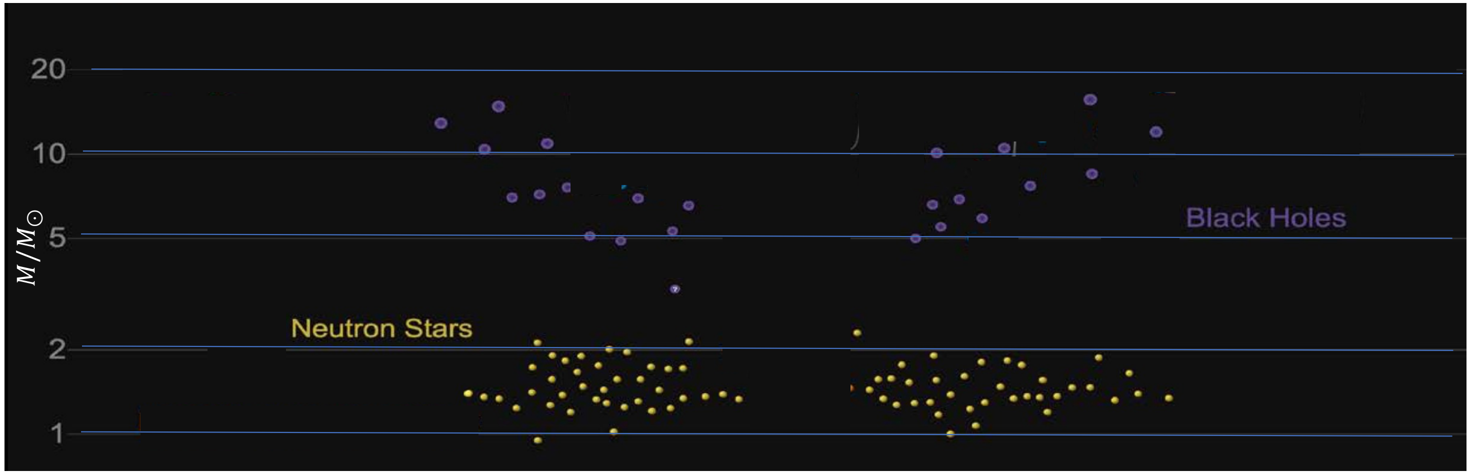

X-ray binaries

Maximal possible rate of accretion.

If the matter accreting onto black hole gets too hot, radiation pressure force

$$F_{rad} = p n_{ph} c \sigma_T = \frac{L}{4\pi R^2 c} \sigma_T$$

would balance the gravity force, so that matter would not be able to fall onto the black hole:

$$F_g = \frac{G_N M m_p}{R^2} \sim \frac{L}{4\pi R^2 c} \sigma_T = F_{rad}$$

This imposes a limit onto luminosity:

$$L < L_{Edd} = \frac{4\pi c G_N M m_p}{\sigma_T} \simeq 10^{38} \left[\frac{M}{M_\odot}\right] \frac{\mathrm{erg}}{\mathrm{s}}$$

(Eddington limit). The temperature of the accretion flow (black body radiation)

$$L \sim L_\odot \left(\frac{R}{R_\odot}\right)^2 \left(\frac{T}{T_\odot}\right)^4$$

Is limited to

$$T \sim T_\odot \left(\frac{L}{L_\odot}\right)^{\frac{1}{4}} \left(\frac{R}{R_\odot}\right)^{-\frac{1}{2}} \sim 3\times 10^7 \left(\frac{M}{M_\odot}\right)^{-\frac{1}{4}} \mathrm{K}$$

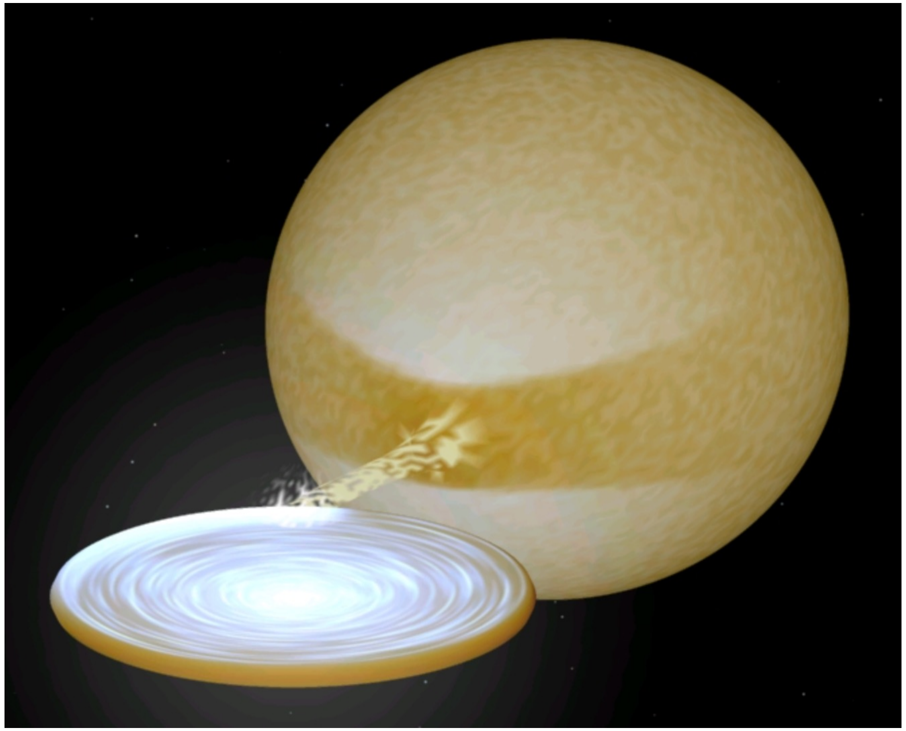

For stellar mass black hole, the black body emission is in the X-ray band, supermassive black holes have accretion flows emitting in the UV.

X-ray binaries

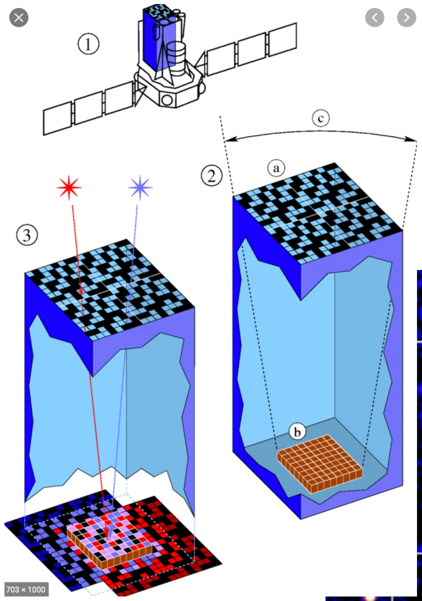

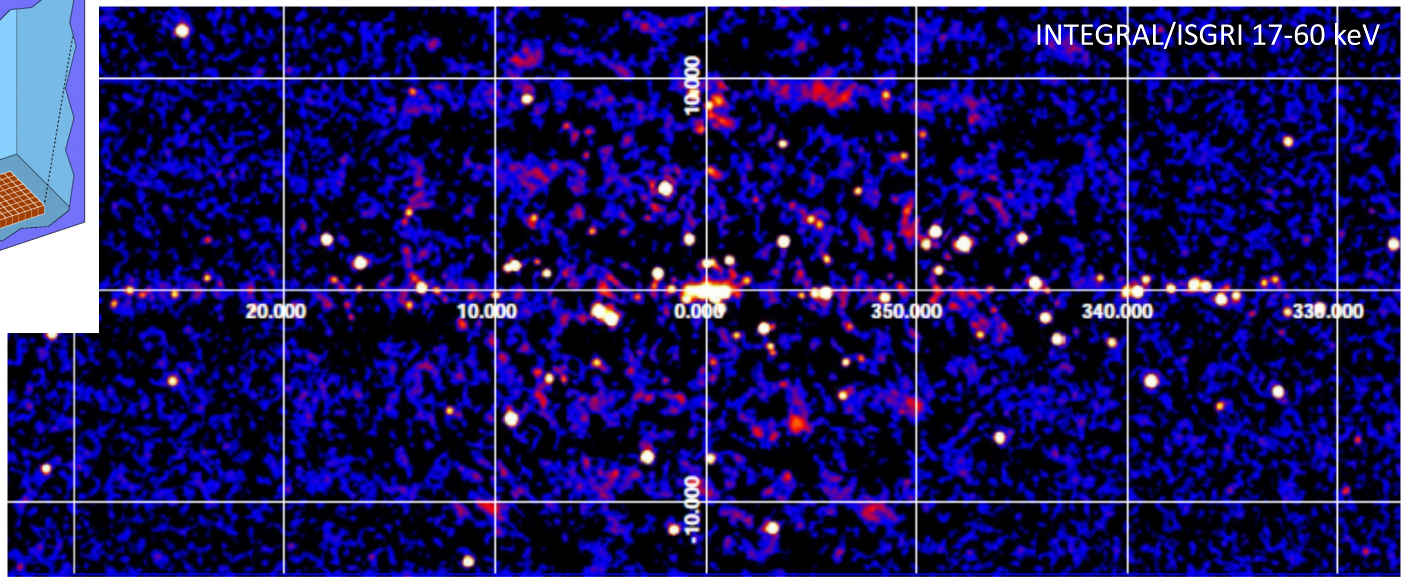

Most of X-ray sources in the Milky Way are X-ray binaries.

Microquasars

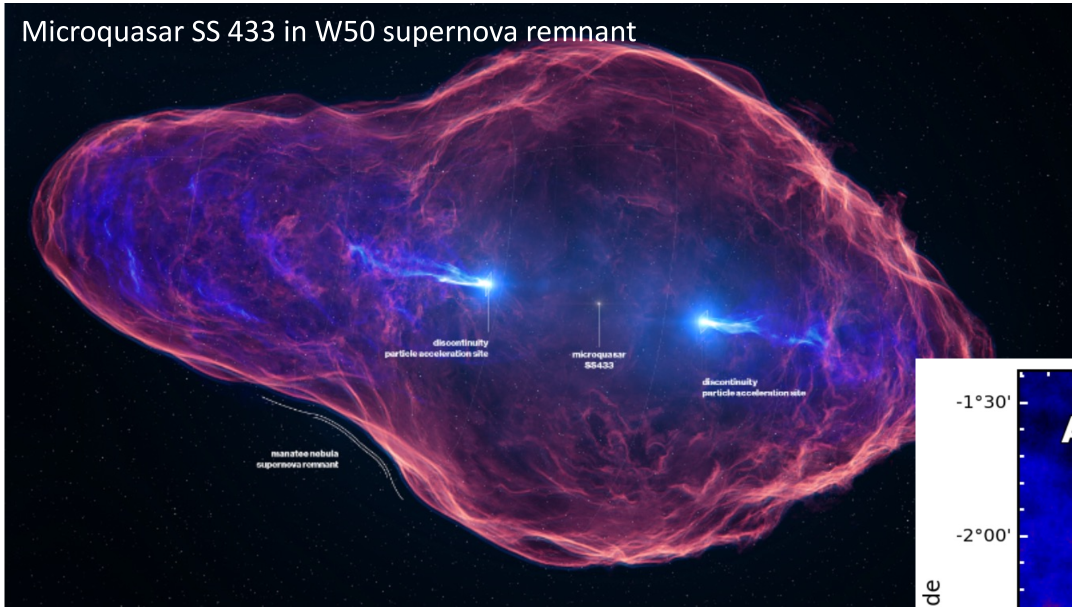

Similar to AGN, some stellar mass black holes operate particle accelerators and eject jets of high-energy particles.

Mildly-relativistic jets penetrate in circumstellar medium and form shocks. Particle acceleration most probably happens in the shocks.

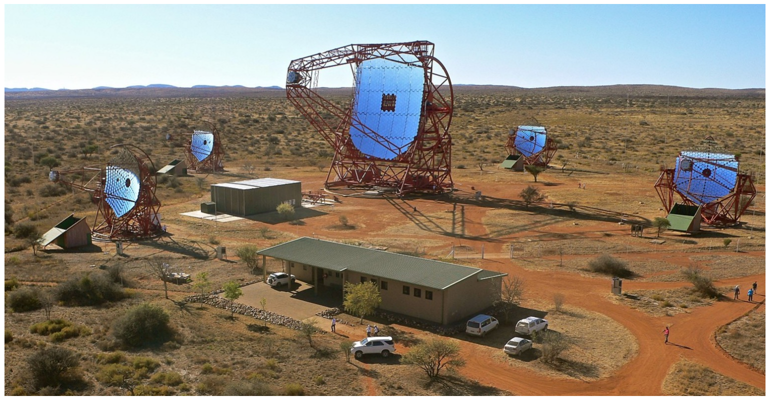

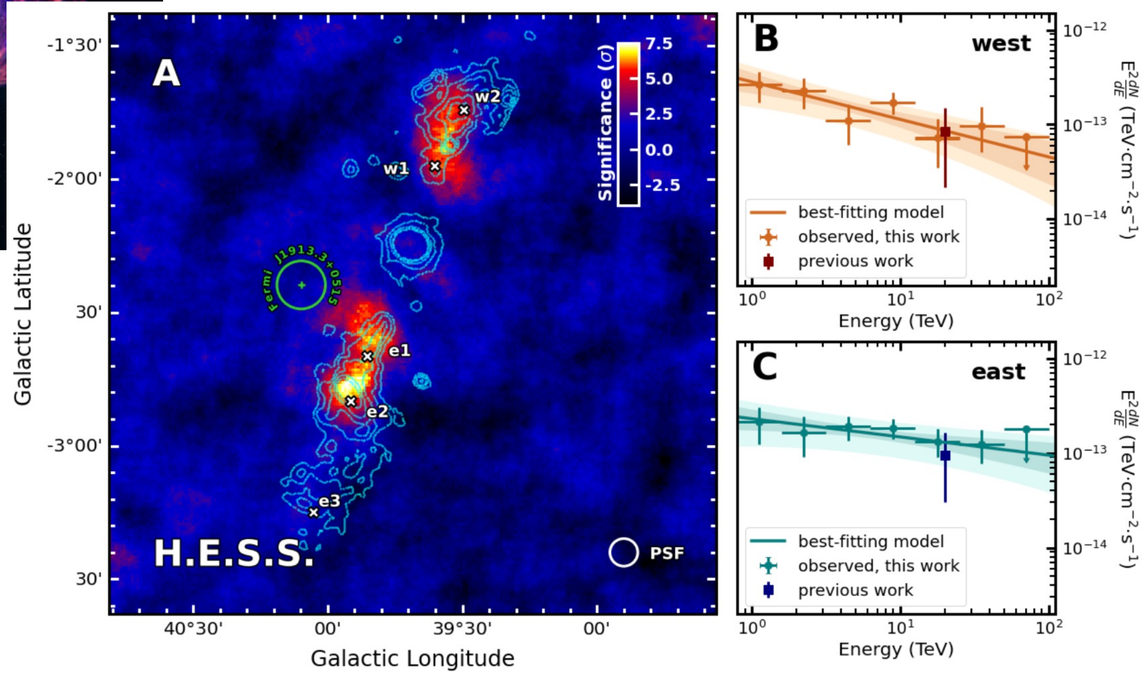

Gravitational waves from stellar mass black holes

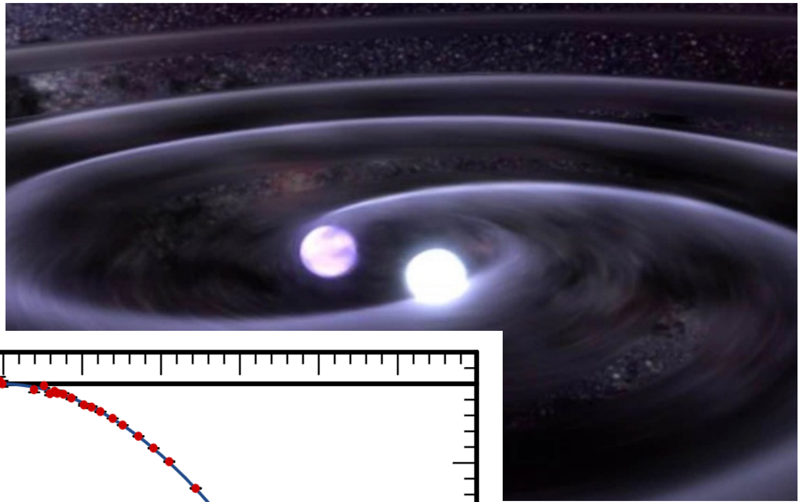

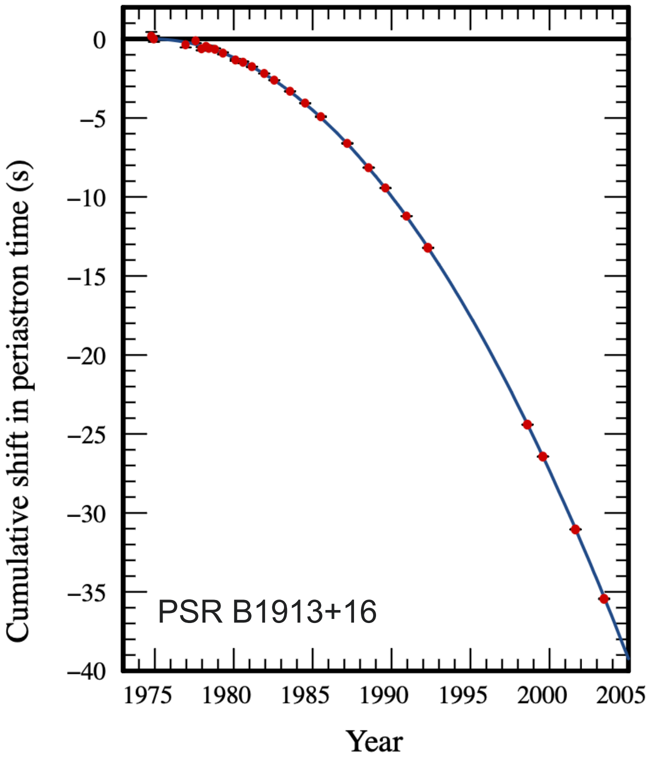

Neutron stars in compact binary systems can have rotation periods as short as

$$P = \sqrt{\frac{2\pi\, R^3}{G_N M}} \simeq 5 \left[\frac{M}{10^1 M_\odot}\right]^{-\frac{1}{2}} \left[\frac{R}{10^7\ \mathrm{cm}}\right]^{\frac{3}{2}} \mathrm{ms}; \quad \nu = P^{-1}$$

Just before the merger (when the binary orbit size is about the sum of the radii of two neutron stars).

Orbits of close compact object binaries shrink because of emission of gravitational radiation. The power of the gravitational wave emission is determined by the time variability of the quadrupole moment of mass distribution:

$$I = \frac{G_N}{5c^5}\left(\Sigma \dddot{Q}_{jk} \dddot{Q}^{jk} - \frac{1}{3}\, \dddot{Q}^2\right)$$

$Q^{jk} = \int \rho x^j x^k d^3 x$ is the quadrupole moment of the mass distribution (ρ is the mass density). The amplitude of gravitational waves as

$$h \sim \frac{\Delta x}{x} \sim \frac{2G_N}{c^4 D}\ \ddot{Q}$$

($\Delta x/x$ is the relative change of the distance scales at the measurement location at the distance D form the source).

(notice analogy with the dipole radiation in electromagnetism: $I = \frac{2}{3}\ddot{\vec{d}}^2$
$d^i = \int q\, x^i d^3 x$, where q is the charge density).

Gravitational waves from stellar mass black holes

LIGO gravitational wave detector in USA

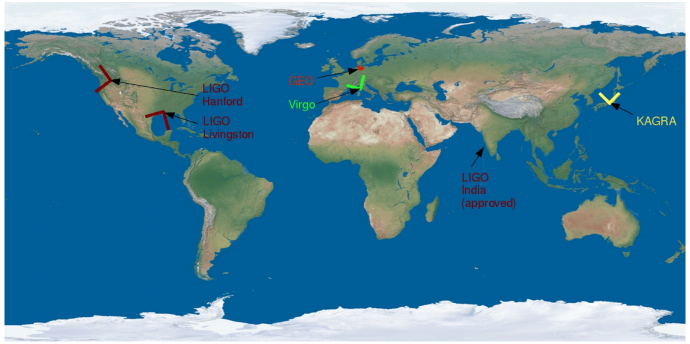

Worldwide network of gravitational wave detectors

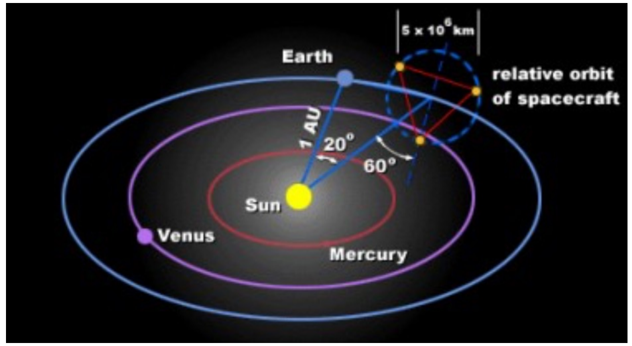

Space-based gravitational wave detector LISA (a Large mission project of ESA, to be launched in 2031)

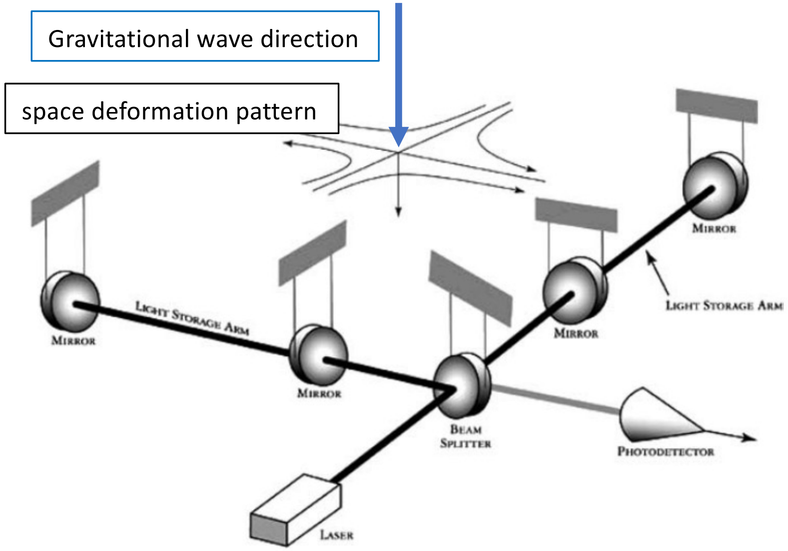

Gravitational wave detectors use interferometer technique to measure small variations of distances between bodies induced by the passage of the wave (small perturbations of the flat Minkovski space-time metric $\eta_{\mu\nu}$:

$$g_{\mu\nu} = \eta_{\mu\nu} + h_{\mu\nu}$$

$h_{\mu\nu} \ll 1.$

The length of interferometer's arm is $x = \int_0^L (1+h)dx = x + \Delta x$ changes if $h \neq 0$.

This technique allows to measure $h \sim 10^{-21}$ for the waves of $\nu \sim 1$ kHz frequency with interferometers with of the size $L \sim 1$ km.

Gravitational waves from stellar mass black holes

A sample of $\sim 10^2$ "GW bursts" has been detected in three runs (O1, O2, O3) of LIGO-VIRGO.
Most of them are mergers of two black holes, rather than two neutron stars. The "O4" run is on-going now (2024).

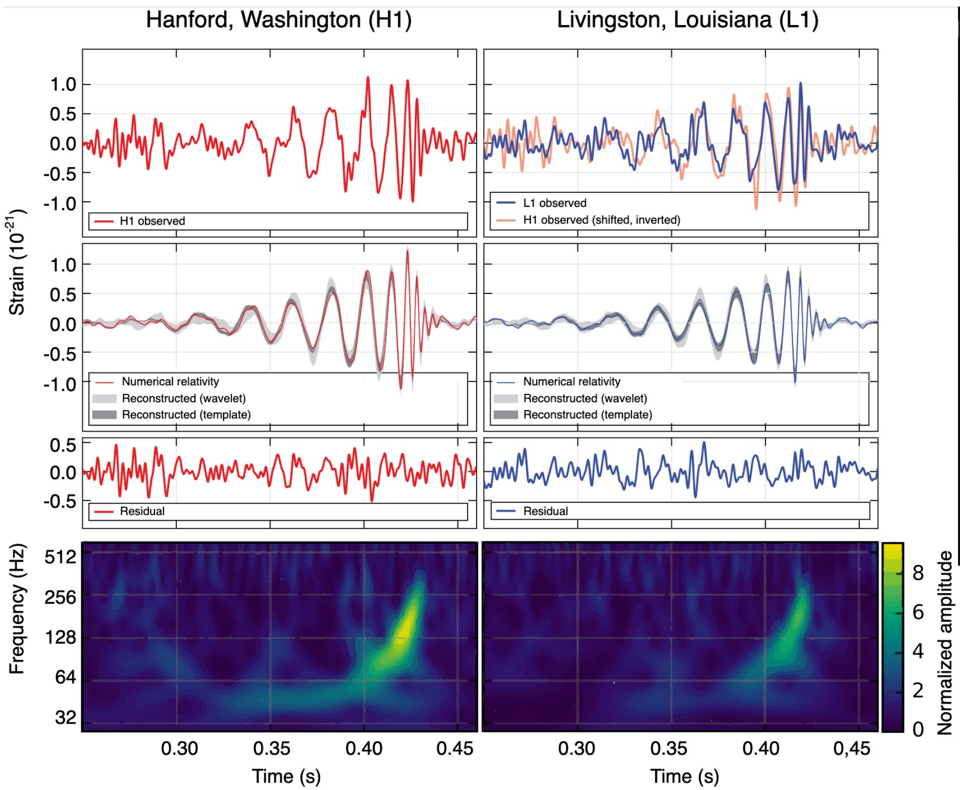

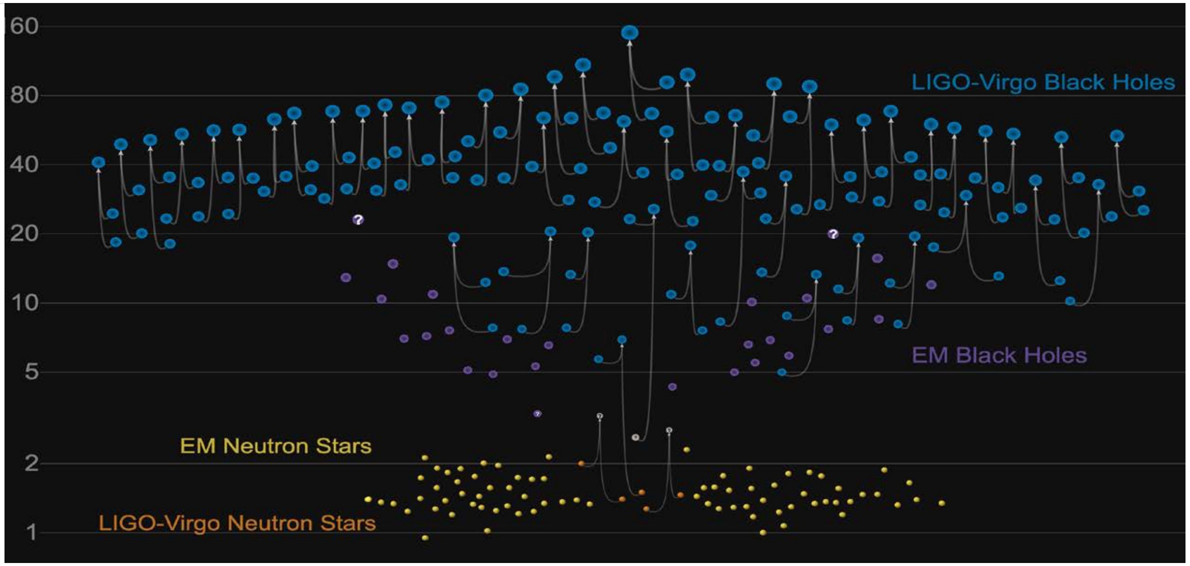

GW150914

Gravitational waves from supermassive black holes?

Passage of gravitational waves distorts the pattern of arrival time of milli-second pulsars by changing the distance to the sources. Measurement of timing residuals allows to detect gravitational waves with extremely low frequency, down to nHz (low frequency end is determined by the duration of timing monitoring, currently ~ 10 yr scale).

PTA collaborations (NANOGrav, EPTA, PPTA) have reported in 2023 evidence for "stochastic gravitational wave background" in the 10^{-8} Hz frequency range. Its origin can be from a population of binary supermassive black holes:

$$P = \sqrt{\frac{2\pi R^3}{G_N M}} \simeq 5 \left[\frac{M}{10^7 M_\odot}\right]^{-\frac{1}{2}} \left[\frac{R}{10^{16}\ \mathrm{cm}}\right]^{\frac{3}{2}} \mathrm{yr}; \quad \nu = P^{-1}$$

Otherwise, it may originate from the Early Universe.

Gravitational waves from supermassive black holes?

Passage of gravitational waves distorts the pattern of arrival time of milli-second pulsars by changing the distance to the sources. Measurement of timing residuals allows to detect gravitational waves with extremely low frequency, down to nHz (low frequency end is determined by the duration of timing monitoring, currently ~ 10 yr scale).

NANOGrav Collab. ‘20 (arXiv:2009.04496)
PPTA Collab. ’21 (arXiv:2107.12112)
EPTA Collab. ‘21 (arXiv:2110.13184)
IPTA Collab. ‘22 (arXiv:2201.03980

All PTA collaborations (NANOGrav, EPTA, PPTA, collaborating within “International” PTA, IPTA) have reported evidence for “common stochastic process” detectable in timing residuals of many pulsars. This is consistent with existence of stochastic gravitational wave background, possibly originating from binary supermassive black hole systems in centers of galaxies.

Alternatively, the background may originate from the “early Universe” (cosmological phase transition associated to quark confinement).

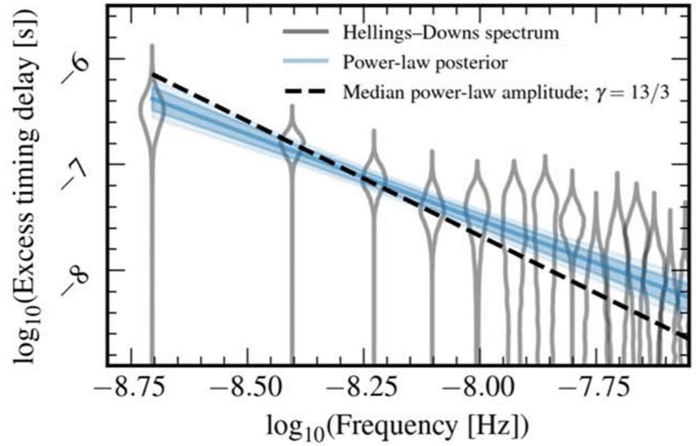

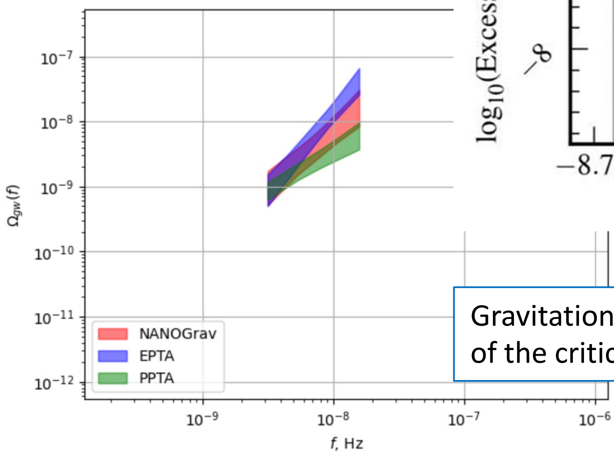

Gravitational wave energy density in units of the critical density of the Universe.